

## Blue compact galaxies and the primordial $^4\text{He}$ abundance

Trinh Xuan Thuan

*Astronomy Department, University of Virginia, P.O. Box 3818,  
University Station, Charlottesville, VA 22903, USA*

Yuri I. Izotov

*Main Astronomical Observatory, Ukrainian National Academy of  
Sciences, Goloseevo, Kiev 03680, Ukraine*

### Abstract.

Blue compact galaxies (BCG) are ideal objects in which to derive the primordial  $^4\text{He}$  abundance because they are chemically young and have not had a significant stellar He contribution. We discuss a self-consistent method which makes use of all the brightest He I emission lines in the optical range and solves consistently for the electron density of the He II zone. We pay particular attention to electron collision and radiative transfer as well as underlying stellar absorption effects which may make the He I emission lines deviate from their recombination values. Using a large homogeneous sample of 45 low-metallicity H II regions in BCGs, and extrapolating the Y-O/H and Y-N/H linear regressions to O/H = N/H = 0, we obtain  $Y_p = 0.2443 \pm 0.0015$ , in excellent agreement with the weighted mean value  $Y_p = 0.2452 \pm 0.0015$  obtained from the detailed analysis of the two most metal-deficient BCGs known, I Zw 18 and SBS 0335-052. The derived slope  $dY/dZ = 2.4 \pm 1.0$  is in agreement with the value derived for the Milky Way and with simple chemical evolution models with homogeneous outflows. Adopting  $Y_p = 0.2452 \pm 0.0015$  leads to a baryon-to-photon ratio of  $(4.7_{-0.8}^{+1.0}) \times 10^{-10}$  and to a baryon mass fraction in the Universe  $\Omega_b h_{50}^2 = 0.068_{-0.012}^{+0.015}$ , consistent with the value derived from the primordial D abundance of Burles & Tytler (1998).

## 1. Introduction

Blue compact galaxies (BCG) are low-luminosity ( $M_B \gtrsim -18$ ) systems which are undergoing an intense burst of star formation in a very compact region (less than 1 kpc) which dominates the light of the galaxy (Figure 1) and which shows blue colors and a HII region-like emission-line optical spectrum (Figure 2). BCGs are ideal laboratories in which to measure the primordial  $^4\text{He}$  abundance because of several reasons:

- 1) With an oxygen abundance O/H ranging between 1/50 and 1/3 that of the Sun, BCGs are among the most metal-deficient gas-rich galaxies known. Their gas has not been processed through many generations of stars, and thus

Figure 1. Slit orientations superposed on *HST* archival *V* images of I Zw 18 and SBS 0335–052. The slit orientation of I Zw 18 is chosen in such a way as to get spectra of the SE and NW components as well as of the C component to the NW of the main body of the galaxy. The spatial scale is  $1'' = 49$  pc in the case of I Zw 18 and is  $1'' = 257$  pc in the case of SBS 0335–052.

best approximates the pristine primordial gas. Izotov & Thuan (1999) have argued that BCGs with O/H less than  $\sim 1/20$  that of the Sun may be genuine young galaxies. Their argument is based on the observed constancy and very small scatter of the C/O and N/O ratios in extremely metal-deficient BCGs with  $12 + \log \text{O}/\text{H} \lesssim 7.6$ , which they interpret as implying that the C and N in these galaxies have been made in the same massive stars ( $M \gtrsim 9 M_{\odot}$ ) which manufactured O, and that intermediate-mass stars ( $3 M_{\odot} \lesssim M \lesssim 9 M_{\odot}$ ) have not had time to release their nucleosynthetic products. Since the main-sequence lifetime of a  $9 M_{\odot}$  star is  $\sim 40$  Myr, Izotov & Thuan (1999) suggest that very metal-deficient BCGs are younger than  $\sim 100$  Myr. Thus the primordial Helium mass fraction  $Y_p$  can be derived accurately in very metal-deficient BCGs with only a small correction for Helium made in stars.

2) Because of the relative insensitivity of  ${}^4\text{He}$  production to the baryonic density of matter,  $Y_p$  needs to be determined to a precision better than 5% to provide useful cosmological constraints. This precision can in principle be achieved by using BCGs because their optical spectra show several He I recombination emission lines and very high signal-to-noise ratio emission-line spectra with moderate spectral resolution of BCGs can be obtained at large telescopes (4 m class or larger) coupled with efficient and linear CCD detectors with a relatively modest investment of telescope time. The theory of nebular emission is well understood and the theoretical He I recombination coefficients calculated by Brocklehurst (1972) and Smits (1996) are well known enough to allow to convert He emission-line strengths into abundances with the desired accuracy.

## 2. The primordial He abundance from extrapolation of the Y-O/H and Y-N/H linear regressions

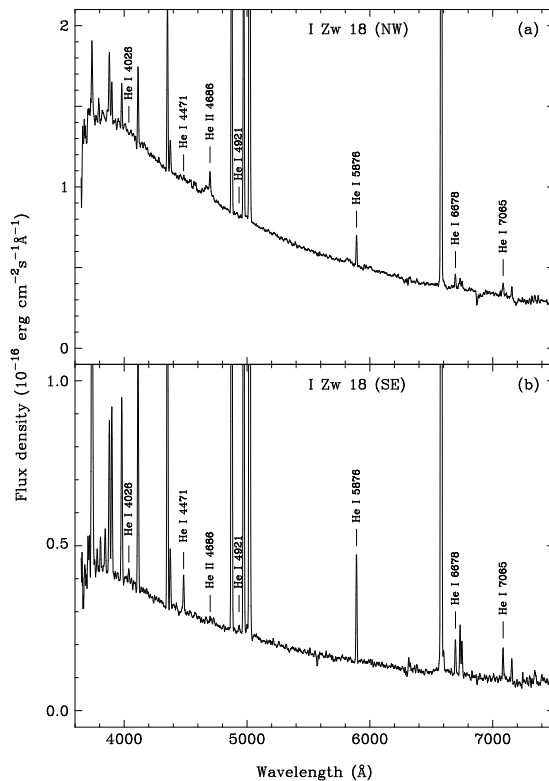


Figure 2. The  $0''.6 \times 1''.5$  aperture MMT spectra of the brightest parts of the NW and the SE components of I Zw 18. The spectrum of the SE component is extracted at the angular distance of  $5''.4$  from the NW component. The positions of He I lines are marked. Note that all marked He I lines in the spectrum of the SE component are in emission while the two He I  $\lambda 4026$  and  $\lambda 4921$  lines are in absorption and the He I  $\lambda 4471$  emission line is barely detected in the spectrum of the NW component.

## 2.1. A new large sample of Blue Compact Galaxies

Peimbert & Torres-Peimbert (1974, 1976) first noted the correlation between He and O abundances in a small sample of dwarf magellanic irregulars and BCGs, and they proposed to determine  $Y_p$  by linear extrapolation of the correlation to  $O/H = 0$ . Later, Pagel, Terlevich & Melnick (1986) proposed to use also the  $Y-N/H$  correlation for the determination of  $Y_p$ , to take into account the temporary local excess of helium and nitrogen due to pollution by winds from massive stars. Many attempts at determining  $Y_p$  have been made, using the  $Y$  versus  $O/H$  and  $Y$  versus  $N/H$  correlations on various samples of dwarf irregulars and BCGs (e.g. Pagel et al. 1992, Izotov, Thuan & Lipovetsky (1994, 1997, hereafter ITL94 and ITL97; Olive, Steigman & Skillman 1997, hereafter OSS97; Izotov & Thuan 1998ab, hereafter IT98ab).

Before our work, the largest, most accurate and consistent published data set was by Pagel et al. (1992). Their observations were reduced in a uniform manner and they paid careful attention to such points as the correction for the unseen neutral helium and electron collisional effects which may make some He I lines deviate from their recombination values. Pagel et al. (1992) obtained  $Y_p = 0.228 \pm 0.005$ , below the limit set by the standard hot big bang model of nucleosynthesis (SBBN) and consistent with it only at the  $2\sigma$  level. This prompted us to consider obtaining another measurement of  $Y_p$  from an independent data set with as high or better precision to test SBBN.

Starting in 1993, we embarked on a large-scale program to obtain high signal-to-noise ratio spectra for a relatively large sample of BCGs assembled from several objective-prism surveys: the First Byurakan or Markarian survey (Markarian et al. 1989), the Second Byurakan Survey (SBS, Izotov et al. 1993) and the University of Michigan survey (Salzer, MacAlpine & Boroson 1989). The SBS sample was particularly interesting because it contained about a dozen BCGs with O/H less than 1/15 of  $(\text{O}/\text{H})_{\odot}$ , more than doubling the number of such known low-metallicity BCGs. The total sample consists of 45 H II regions in 42 BCGs. The data have been published in a series of papers in the *Astrophysical Journal*: ITL94, ITL97 and IT98ab.

## 2.2. Methodology

There are a number of features which distinguish our work from previous efforts in determining the primordial He abundance. Our methodology is described in detail in ITL94, ITL97, and IT98ab.

1) We have observed all the galaxies in our sample with the same telescopes (the Kitt Peak 4 m and 2.1 m telescopes) and instrumental set up, and the data were all reduced in a homogeneous way. This differs from OSS97, for example, which used a more heterogeneous sample of BCGs observed by different observers on different telescopes, with some of the data obtained many years ago with nonlinear detectors. A uniform sample is essential to minimize as much as possible the artificial scatter introduced by assembling different data sets reduced in different ways.

2) To derive the He mass fraction, previous authors use mainly one He emission line, He I 6678. Correction to this line's intensity is usually made only for one effect, electron collisional enhancement. This correction is usually carried out adopting the electron density derived from the [S II] 6717/6731 emission-line ratio. The approach just described has several shortcomings. The metastability of the  $2^3\text{S}$  state of He I can also lead to possible radiative transfer effects (also called fluorescence effects) in the triplet lines which may be enhanced at the expense of the He I 3889 line (Robbins 1968). When a single He I emission line is used, one cannot distinguish between electron collisional and radiative transfer effects. Thus, fluorescent enhancement is neglected, while it may be important. Furthermore, at the low electron number densities  $N_e$  which often characterize the HII regions in BCGs, the determination of  $N_e$  from [S II] emission lines is very uncertain. In the majority of cases,  $N_e$  is arbitrarily set to  $100 \text{ cm}^{-3}$ . This assumption can lead to artificially low He abundance, as in the case of the southeast component of I Zw 18 where the true  $N_e$  is only  $\sim 10 \text{ cm}^{-3}$  (Izotov et al. 1999). More importantly, setting  $N_e(\text{He II})$  equal to  $N_e(\text{S$

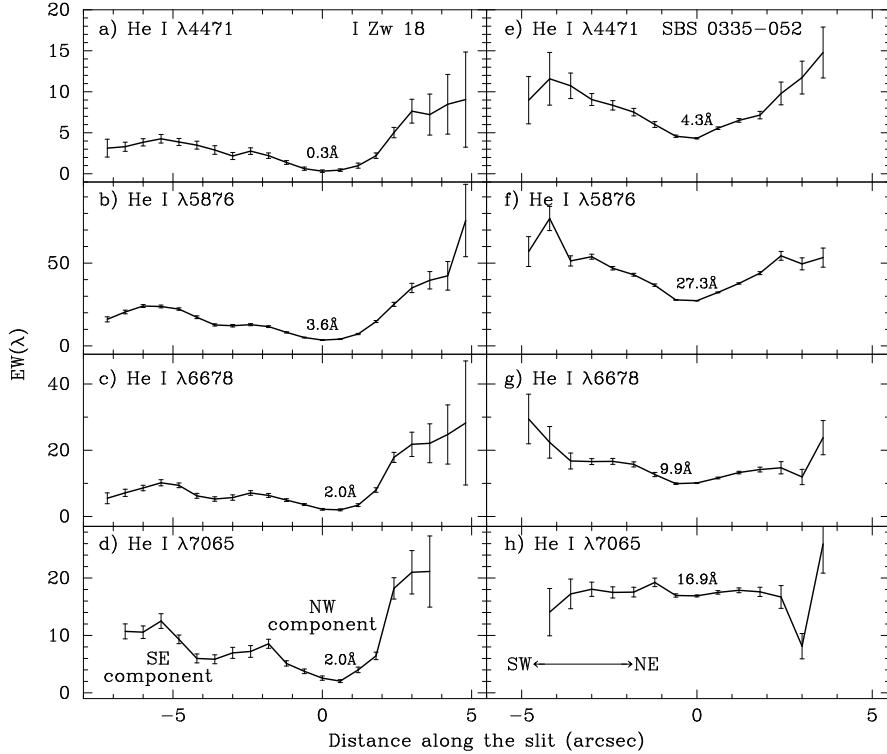


Figure 3. The spatial distributions of the He I nebular emission line equivalent widths in I Zw 18 (left panel) and in SBS 0335–052 (right panel). The error bars are  $1\sigma$  deviations. The value of the minimum equivalent width for each He I emission line is given.

II) is not physically reasonable as the  $S^+$  and  $He^+$  regions are not expected to coincide, given the large difference in the S I and He I ionization potentials.

To remedy these problems, we have proposed a self-consistent method in which we use all five brightest He I emission-lines in the optical range (the He I 3889, 4471, 5876, 6678 and 7065 lines) and solve simultaneously for  $N_e(\text{He II})$  and the optical depth in the He I 3889 line so that the He I 3889/4471, 5876/4471, 6678/4471 and 7065/4471 line ratios have their recombination values, after correction for both collisional (Kingdon & Ferland 1995) and fluorescent (Robbins 1968) enhancements. The He I 3889 and 7065 lines play an important role because they are particularly sensitive to both optical depth and electron number density.

### 2.3. Underlying stellar absorption

Effects other than collisional and fluorescent enhancements can also change He I line intensities. An important effect is the underlying stellar absorption in He I lines caused by hot OB stars which decreases the intensities of nebular He I lines. This effect is most important for the emission lines with the smallest equivalent widths.

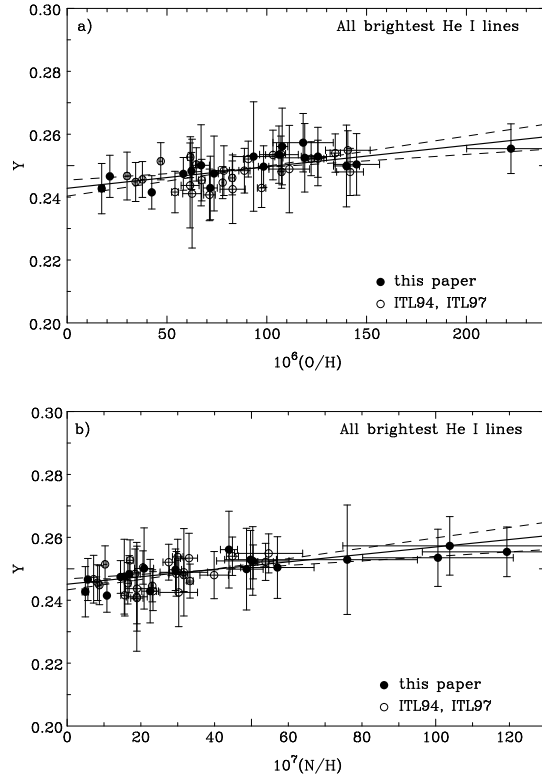


Figure 4. Linear regressions of (a) the helium mass fraction  $Y$  vs. oxygen abundance  $O/H$  and (b) the helium mass fraction  $Y$  vs. nitrogen abundance for our sample of 45 H II regions. The  $Y$ s are derived self-consistently by using the 5 brightest He I emission lines in the optical range. Collisional and fluorescent enhancements, underlying He I stellar absorption and Galactic Na I interstellar absorption are taken into account. Open circles denote data from ITL94 and ITL97 and filled circles are data from IT98ab.  $1\sigma$  alternatives are shown by dashed lines.

The neglect of He I underlying stellar absorption can lead to a severe underestimate of the He mass fraction. One of the most spectacular examples is that of the BCG I Zw18. This object plays a key role in the determination of the primordial He abundance because, with an O/H only 1/50 that of the Sun, it is the most metal-deficient BCG known and has great influence on the derived slopes and intercepts of the Y-O/H and Y-N/H linear regression lines. Figure 2 shows very high signal-to-noise ratio spectrophotometric observations of I Zw 18 obtained with the Multiple Mirror Telescope (MMT), with the slit oriented so as to go through the two main centers of star formation in the BCG, the so-called NW and SE components (Figure 1, left). Comparison of the spectrum of the NW component (Figure 2a) with that of the SE component (Figure 2b) shows clearly that underlying stellar absorption is much more important in the NW than in the SE component: all marked He I lines in the spectrum of the SE component are in emission while the two He I 4026 and 4921 lines are in absorption and the He I 4471 emission line is barely visible in the spectrum of the NW component. Prior to our work, most of the He work relied on measurements of Y in the NW component because of its larger brightness as compared to the SE component (Figure 1, left). This led to a systematic underestimate of Y in I Zw 18. Izotov et al. (1999) derive the implausibly small  $Y(4471) = 0.169 \pm 0.023$  and  $Y(5876) = 0.192 \pm 0.007$  from the He I 4471 and 5876 lines respectively. In addition to underlying stellar absorption, the 5876 line intensity in I Zw 18 is reduced further by absorption from the Galactic interstellar 5890 and 5896 Na I lines.

While the NW component cannot be used for He determination, the SE component is better suited as the influence of underlying stellar absorption on the He I emission line intensities is significantly smaller in this component. This can be seen in the left panel of Figure 3 which shows the spatial distributions of the He I nebular emission-line equivalent widths in I Zw 18: they are systematically larger in the SE component than in the NW one, implying less absorption.

## 2.4. Results

Figure 4 shows the Y-O/H and Y-N/H linear regressions for the whole sample of 45 H II regions in BCGs. The sample includes most of the very metal-deficient BCGs known, including the two most extreme ones, the SE component of I Zw 18 and SBS 0335-052 with O/H about 1/43 that of the Sun. We obtain  $Y_p = 0.2443 \pm 0.0015$  with  $dY/dZ = 2.4 \pm 1.0$  (IT98b). Our  $Y_p$  is considerably higher than those derived by other groups which range from  $0.228 \pm 0.005$  (Pagel et al. 1992) to  $0.234 \pm 0.002$  (OSS97). At the same time, our derived slope is significantly smaller than those of other authors,  $dY/dZ = 6.7 \pm 2.3$  for Pagel et al. (1992) and  $dY/dZ = 6.9 \pm 1.5$  for OSS97. This shallower slope is in good agreement with the value derived from stellar data for the Milky Way's disk and with simple models of galactic evolution of BCGs with well-mixed homogeneous outflows.

## 3. He abundance in the two most metal-deficient blue compact galaxies known

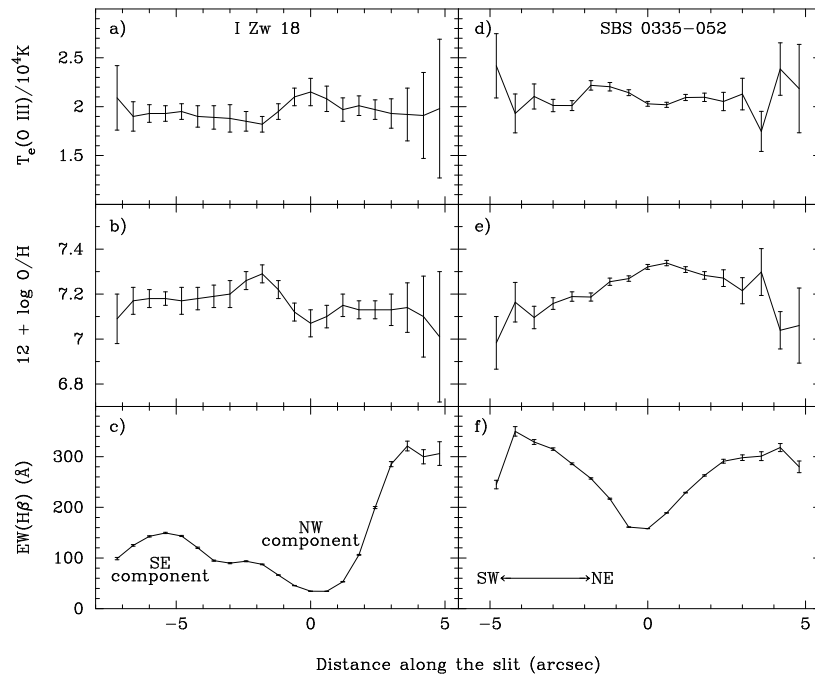


Figure 5. The spatial distributions of the electron temperature  $T_e(\text{O III})$ , oxygen abundance  $12 + \log (\text{O}/\text{H})$ , and the equivalent width  $EW(\text{H}\beta)$  of the  $\text{H}\beta$  emission line in I Zw 18 (left panel) and in SBS 0335-052 (right panel). The error bars are  $1\sigma$  deviations.

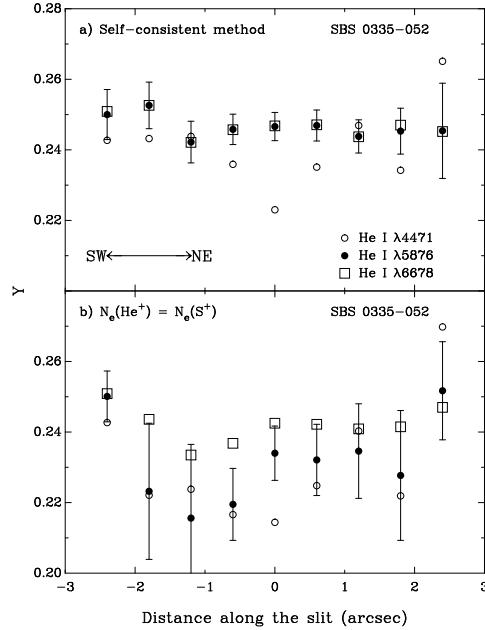


Figure 6. The spatial distributions of the helium mass fractions in SBS 0335–052 derived from the He I  $\lambda 4471$ ,  $\lambda 5876$  and  $\lambda 6678$  emission line intensities. The intensities of the He I emission lines in Figure 6a are corrected for fluorescent and collisional enhancement with an electron number density  $N_e(\text{He II})$  and an optical depth  $\tau(\lambda 3889)$  derived self-consistently from the observed He I  $\lambda 3889$ ,  $\lambda 4471$ ,  $\lambda 5876$ ,  $\lambda 6678$  and  $\lambda 7065$  emission line intensities. The intensities of the He I emission lines in Figure 6b are corrected only for collisional enhancement with an electron number density  $N_e(\text{S II})$ . The  $1\sigma$  error bars are shown only for the He mass fraction derived from the He I  $\lambda 5876$  emission line. They are larger in Figure 6b because of the large uncertainties in the determination of  $N_e(\text{S II})$ .

### 3.1. I Zw 18 and SBS 0335–052

Instead of the statistical approach described above, we can also derive the primordial He abundance from accurate measurements of the He abundance in a few objects selected to have very low O/H to minimize the amount of He manufactured in stars.

Izotov et al. (1999) have carried out such a study for the two most metal-deficient BCGs known. I Zw 18 and SBS 0335–052 provide a study in contrast concerning the different physical mechanisms which may modify the He I emission-line intensities. While in I Zw 18, the electron number density is small ( $N_e \lesssim 100 \text{ cm}^{-3}$ ) and collisional enhancement has a minor effect on the derived helium abundance,  $N_e$  is much higher in SBS 0335–052 ( $N_e \sim 500 \text{ cm}^{-3}$  in the central part of the H II region). Additionally, the linear size of the H II region in SBS 0335–052 is  $\sim 5$  times larger than in I Zw 18, suggesting that it may be optically thick for some He I transitions. In fact, both collisional and fluorescent enhancements of He I emission lines play an important role in this galaxy. By contrast, underlying stellar He I absorption is much less important in SBS 0335–052 than in I Zw 18. Since the equivalent widths (EW) of the He I emission lines scale roughly as the  $H\beta$  EWs, it is evident that this is the case from Figures 5c and 5f which show the spatial distribution of  $\text{EW}(H\beta)$  in both BCGs. In SBS 0335–052,  $\text{EW}(H\beta)$  has a lowest value of 160 Å and increases to  $\sim 300$  Å in the outer parts, while in I Zw 18,  $\text{EW}(H\beta)$  is only 34 Å in the center of the NW component. Given equal EWs for He I absorption lines in both BCGs, we may expect the effect of underlying stellar absorption to be  $\sim 5$  times smaller in SBS 0335–052 than in I Zw 18.

To disentangle the various effects which may make the He I emission-line intensities deviate from their recombination values, it is thus essential to use as many He I lines as possible in a self-consistent method as described above. An important and essential check that all corrections have been properly applied is the agreement between the He mass fraction  $Y$  derived independently from each He line. Figure 6 shows the  $Y$ s derived from the 4471, 5876 and 6678 He I emission lines in SBS 0335–052 at different spatial locations. It is clear that the self-consistent method (Figure 6a) gives much better agreement between the different lines. The  $Y$ s derived from the 4471 line are systematically below because only collisional and fluorescence effects have been taken into account and not underlying stellar absorption, and because the 4471 line is more subject to the latter effect. By contrast, there is not very good agreement between the  $Y$ s from different lines when  $N_e(\text{He II})$  is set equal to  $N_e(\text{S II})$  and only collisional enhancement is taken into account (Figure 6b).

### 3.2. Results

Izotov et al. (1999) derive  $Y = 0.243 \pm 0.007$  for the SE component of I Zw 18 in very good agreement with the value found by IT98a and  $Y = 0.2463 \pm 0.0015$  for SBS 0335–052, excluding the He I 4471 line. The weighted mean is then  $Y = 0.2462 \pm 0.0015$ . Using  $dY/dZ = 2.4$  (IT98b), the stellar He contribution is 0.0010, giving a primordial value  $Y_p = 0.2452 \pm 0.0015$ , in excellent agreement with the value  $0.2443 \pm 0.0015$  derived from extrapolation of the  $Y$ -O/H and  $Y$ -N/H regression lines for our large BCG sample. It is, however, higher than

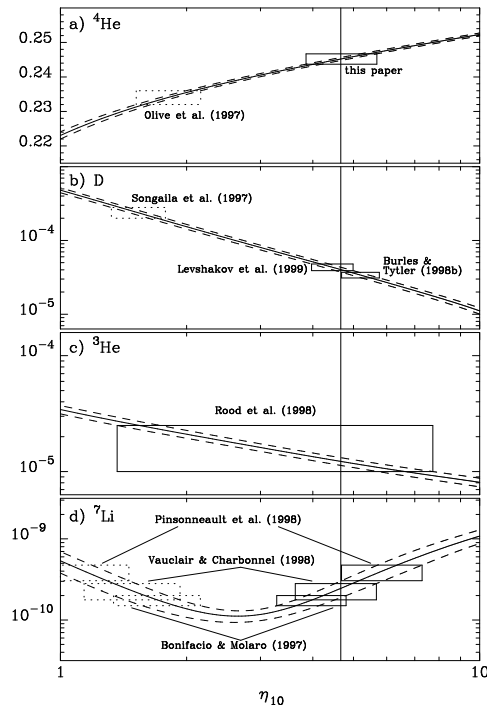


Figure 7. The abundance of (a)  ${}^4\text{He}$ , (b)  $\text{D}$ , (c)  ${}^3\text{He}$  and (d)  ${}^7\text{Li}$  as a function of  $\eta_{10} \equiv 10^{10} \eta$ , where  $\eta$  is the baryon-to-photon ratio, as given by the standard hot big bang nucleosynthesis model. The abundances of  $\text{D}$ ,  ${}^3\text{He}$  and  ${}^7\text{Li}$  are number ratios relative to  $\text{H}$ . For  ${}^4\text{He}$ , the mass fraction  $Y$  is shown. Our value  $Y_p = 0.2452 \pm 0.0015$  gives  $\eta = (4.7^{+1.0}_{-0.8}) \times 10^{-10}$  as shown by the solid vertical line. We show other data with  $1\sigma$  boxes.

the value  $Y_p = 0.2345 \pm 0.0030$  derived by Peimbert & Peimbert (2000) from Magellanic Clouds H II regions. These authors suggest that two systematic effects may cause the disagreement: the presence of neutral hydrogen inside the helium Stromgren sphere and temperature fluctuations in our BCGs.

There is no evidence that the first effect is important in our objects. In our work, we have used the 'radiation softness parameter' of Vilchez & Pagel (1988) to estimate the correction factor for neutral helium and found the fraction of neutral helium to be insignificant ( $\lesssim 2\%$ ) in all our objects, i.e their HII and He II Stromgren spheres are coincident to a very good approximation. This conclusion is corroborated by the detailed modeling of I Zw 18 by Stasinska & Schaerer (1999) who found the amount of neutral Helium to be negligible. On the other hand, they did find the observed  $T_e(\text{OIII})$  to be  $\sim 15\%$  higher than predicted by the photoionization model. Future progress in the determination of the primordial  ${}^4\text{He}$  abundance using BCGs will rely on the discovery of more I Zw 18-like objects and on detailed modeling of very high signal-to-noise ratio and high-spectral resolution spectra of a few very metal-deficient BCGs (those

with O/H less than 1/20 of solar) to look into such systematic effects as those mentioned above.

#### 4. Cosmological implications

Figure 7 shows the primordial abundances of  ${}^4\text{He}$ , D,  ${}^3\text{He}$ , and  ${}^7\text{Li}$  predicted by standard big bang nucleosynthesis theory as a function of the baryon-to-photon number ratio  $\eta$ . The dashed lines are  $1\sigma$  uncertainties in model calculations. The solid boxes show the  $1\sigma$  predictions of  $\eta$  as inferred from our derived primordial abundance of  ${}^4\text{He}$ , and the primordial abundances of D (Levshakov, Kegel & Takahara 1999; Burles & Tytler 1998),  ${}^3\text{He}$  (Rood et al. 1998) and  ${}^7\text{Li}$  (Bonifacio & Molaro 1997; Vauclair & Charbonnel 1998; Pinsonneault et al. 1999). All these determinations are consistent to within  $1\sigma$ , although the most stringent constraint is provided by D. For comparison, we have also plotted the  $Y_p$  derived by OSS97 which is low, partly because underlying stellar absorption was not taken into account in I Zw 18. Their  $Y_p = 0.234$  happens also to be the value obtained by Peimbert & Peimbert (2000) in the Magellanic Clouds. This low value would have been consistent with the primordial D abundance obtained by Songaila et al (1997) which is one order of magnitude higher than the value obtained by Burles & Tytler (1998), except that this high value is now believed to be erroneous.

Our  $Y_p = 0.2452 \pm 0.0015$  value implies a baryon-to-photon number ratio  $\eta = 4.7_{-0.8}^{+1.0} \times 10^{-10}$ . This translates to a baryon mass fraction  $\Omega_b h_{50}^2 = 0.068_{-0.012}^{+0.015}$  where  $h_{50}$  is the Hubble constant in units of  $50 \text{ km s}^{-1} \text{ Mpc}^{-1}$ . For a Hubble constant equal to  $65 \text{ km s}^{-1} \text{ Mpc}^{-1}$ ,  $\Omega_b = 0.040_{-0.007}^{+0.009}$ . Our derived baryonic mass fraction is consistent with the one obtained by analysis of the Ly $\alpha$  forest in a cold dark matter cosmology. Depending on the intensity of diffuse UV radiation, the inferred lower limit is  $\Omega h_{50}^2 = 0.05 - 0.10$  (Weinberg et al. 1997; Bi & Davidsen 1997; Rauch et al. 1997), while Zhang et al. (1998) have derived  $0.03 \leq \Omega h_{50}^2 \leq 0.08$ .

Finally, for the most consistent set of primordial abundances – D from Levshakov et al. (1999), our above value for  ${}^4\text{He}$ , and  ${}^7\text{Li}$  from Vauclair & Charbonnel (1998) – we derive an equivalent number of light neutrino species  $N_\nu = 3.0 \pm 0.3$  ( $2\sigma$ ) (Izotov et al. 1999).

**Acknowledgments.** We thank the partial financial support of NSF grant AST-96-16863 and an IAU Travel grant. We acknowledge useful conversations with M. Peimbert and B. Pagel and thank the organizers for a stimulating meeting in a superb locale.

#### References

- Bi, H., & Davidsen, A. F. 1997, ApJ, 479, 523
- Bonifacio, P. & Molaro, P. 1997, MNRAS, 285, 847
- Brocklehurst, M. 1972, MNRAS, 157, 211
- Burles, S., & Tytler, D. 1998a, ApJ, 507, 732 1998, Phys. Rev. D, 58, 063506
- Izotov, Y. I., & Thuan, T. X. 1998a, ApJ, 500, 188 (IT98a)

- . 1998b, *ApJ*, 497, 227 (IT98b)
- . 1999, *ApJ*, 511, 639
- Izotov, Y. I., Thuan, T. X., & Lipovetsky, V. A. 1994, *ApJ*, 435, 647 (ITL94)
- . 1997, *ApJS*, 108, 1 (ITL97)
- Izotov, Y. I., Lipovetsky, V.A., Guseva, N.G., Kniazev, A. Y., Neizvestny, S. I. & Stepanian, J. A. 1993, *Astron. Astrophys. Trans.*, 3, 193
- Izotov, Y. I., Chaffee, F. H., Foltz, C. B., Green, R. F., Guseva, N. G., Thuan, T. X. 1999, *ApJ*, 527, 757
- Kingdon, J., & Ferland, G. J. 1995, *ApJ*, 442, 714
- Levshakov, S. A., Kegel, W. H., & Takahara, F. 1998, *MNRAS*, 302, 707
- Markarian, B. E., Lipovetsky, V.A., Stepanian, J.A., Erastova, L. K., & Shapovalova, A. I. 1989, *Commun. Special Astrophys. Obs.*, 62, 5
- Olive, K. A., Skillman, E. D., & Steigman, G. 1997, *ApJ*, 483, 788 (OSS97)
- Pagel, B. E. J., Simonson, E. A., Terlevich, R. J., & Edmunds, M. G. 1992, *MNRAS*, 255, 325
- Pagel, B. E. J., Terlevich, R. J., & Melnick, J. 1986, *PASP*, 98, 1005
- Peimbert, M., & Torres-Peimbert, S. 1974, *ApJ*, 193, 327
- . 1976, *ApJ*, 203, 581
- Peimbert, M. & Peimbert, A. 2000, this volume
- Pinsonneault, M. H., Walker, T. P., Steigman, G., & Narayanan, V. K. 1999, *ApJ*, 527, 180
- Rauch, M., Miralda-Escudé, J., Sargent, W. L. W., Barlow, T. A., Weinberg, D. H., Hernquist, L., Katz, N., Cen, R., & Ostriker, J. P. 1997, *ApJ*, 489, 7
- Robbins, R. R. 1968, *ApJ*, 151, 511
- Rood, R. T., Bania, T. M., Balsler, D. S., & Wilson, T. L. 1998, *Space Sci. Rev.*, 84, 185
- Salzer, J. J., MacAlpine, G. M., & Boroson, T. A. 1989, *ApJS*, 70, 447
- Smits, D. P. 1996, *MNRAS*, 278, 683
- Songaila, A., Wampler, E. J., & Cowie, L. L. 1997, *Nature*, 385, 137
- Stasińska, G., & Schaerer, D. 1999, *A&A*, 351, 72
- Vauclair, S., & Charbonnel, C. 1998, *ApJ*, 502, 372
- Vílchez, J. M., & Pagel, B. E. J. 1988, *MNRAS*, 231, 257
- Weinberg, D. H., Miralda-Escudé, J., Hernquist, L., & Katz, N. 1997, *ApJ*, 490, 564
- Zhang, Y., Meiksin, A., Anninos, P., & Norman, M. L. 1998, *ApJ*, 495, 63

This figure "thuan\_fig1a.jpg" is available in "jpg" format from:

<http://arxiv.org/ps/astro-ph/0003234v1>

This figure "thuan\_fig1b.jpg" is available in "jpg" format from:

<http://arxiv.org/ps/astro-ph/0003234v1>